Low-energy physics of three-orbital impurity model with Kanamori interaction

Alen Horvat,[1] Rok Žitko,[1,2] and Jernej Mravlje[1]
[1]*Jožef Stefan Institute, Jamova 39, Ljubljana, Slovenia*
[2]*Faculty of Mathematics and Physics, University of Ljubljana, Jadranska 19, Ljubljana, Slovenia*
(Received 24 June 2016; revised manuscript received 3 October 2016; published 19 October 2016)

We discuss the low-energy physics of the three-orbital Anderson impurity model with the Coulomb interaction term of the Kanamori form which has orbital SO(3) and spin SU(2) symmetry and describes systems with partially occupied t_{2g} shells. We focus on the case with two electrons in the impurity that is relevant to Hund's metals. Using the Schrieffer-Wolff transformation we derive an effective Kondo model with couplings between the bulk and impurity electrons expressed in terms of spin, orbital, and orbital quadrupole operators. The bare spin-spin Kondo interaction is much smaller than the orbit-orbit and spin-orbital couplings or is even ferromagnetic. Furthermore, the perturbative scaling equations indicate faster renormalization of the couplings related to orbital degrees of freedom compared to spin degrees of freedom. Both mechanisms lead to a slow screening of the local spin moment. The model thus behaves similarly to the related quantum impurity problem with a larger SU(3) orbital symmetry (Dworin-Narath interaction) where this was first observed. We find that the two problems actually describe the same low-energy physics since the SU(3) symmetry is dynamically established through the renormalization of the splittings between the orbital and quadrupole coupling constants to zero. The perturbative renormalization group results are corroborated with the numerical-renormalization group (NRG) calculations. The dependence of spin Kondo temperatures and orbital Kondo temperatures as a function of interaction parameters, the hybridization, and the impurity occupancy is calculated and discussed.

DOI: 10.1103/PhysRevB.94.165140

I. INTRODUCTION

The theoretical work of recent years has led to a considerably better understanding of the origin of electronic correlations in materials with wide bands and relatively weak Coulomb interactions, such as iron-based superconductors and ruthenates. Based on the dynamical mean-field theory calculations (DMFT) [1] it has been realized that a small multiplet splitting coming from the Hund's rule part of the Coulomb interaction ($J \ll U < W$, with W the bandwidth, U Hubbard interaction) has drastic effects at low-energy scales [2–6]. This has important consequences for the physics of these materials that are hence being referred to as the Hund's metals [6–9].

Impurity models play a major role in the DMFT studies since the problem of the bulk is mapped to a problem of a quantum impurity embedded in a self-consistently determined bath. It is interesting to note that whereas in the single-orbital setting the relevant impurity problem was well explored [10] prior to the development of the DMFT, this is not the case for multiorbital systems where the DMFT calculations preceded [2–6] the detailed investigation of the impurity models, upon which those calculations are based. The discovery of the strong influence of the Hund's rule coupling within the DMFT has encouraged studies of multiorbital effects also for adatoms on metal surfaces. [11,12]

In this paper we study the three-orbital impurity problem with Kanamori interaction,

$$H_{\mathrm{imp}} = \frac{1}{2}(U - 3J)N_d(N_d - 1) - 2J\mathbf{S}^2 - \frac{J}{2}\mathbf{L}^2, \quad (1)$$

relevant, for instance, to the DMFT description of a transition-metal oxide with partially occupied t_{2g} shells. In three-orbital systems, the physics of Hund's metals occurs at occupancy $N_d = 2$ [13]. $\mathbf{L}$,$\mathbf{S}$ are the orbital moment and spin operators, respectively. The Hamiltonian in Eq. (1) has a SU(2) spin and SO(3) orbital symmetry. The low-energy properties of the model defined by Eq. (1) have not been studied so far.

The effects of the Hund's rule coupling were explored for several simpler (mostly two-orbital) models [14–22]. The common conclusion of these works is that the Hund's rule coupling suppresses the Kondo temperature through reduced exchange coupling of the low-lying impurity spin degrees of freedom with conduction electrons.

More recently, a Dworin-Narath (DN) impurity model [23] was studied [24–26]. The DN model is described in terms of the simplified interaction Hamiltonian,

$$H_{\mathrm{imp}} = \frac{1}{2}(U - 3J)N_d(N_d - 1) - 2J\mathbf{S}^2, \quad (2)$$

which is similar to Eq. (1), but without the orbital part of the Hund's interaction, $(J/2)\mathbf{L}^2$. The DN model has a higher SU(3) orbital symmetry and different fixed points. This work has led to important qualitative insights into the physics of Hund's metal. Namely, Refs. [24,25] derived a Kondo Hamiltonian with a SU(M) orbital and SU(N) spin symmetry and argued that the key property is that the spin-spin Kondo coupling is ferromagnetic (or small) and that a two-stage screening of spin and orbital degrees of freedom occurs (see also an earlier pioneering study [27]). In Ref. [25] a renormalization group (RG) analysis stressed the importance of different spin and orbital degeneracy. These findings were corroborated by the numerical-renormalization-group (NRG) study in Ref. [26].

Given the deep implications of these results it is important to investigate the problem for the more realistic interaction term that is actually used in the DMFT calculations. In this paper we investigate the low-energy physics of the Anderson impurity model (AIM) with Kanamori interaction at occupancy close to $N_d = 2$, which is relevant to Hund's

metals. We derive the corresponding Kondo Hamiltonian using the Schrieffer-Wolff transformation. The distinction between the Kanamori and the Dworin-Narath Hamiltonian is found to become asymptotically irrelevant: At low energies, the orbital SO(3) symmetry is dynamically enlarged to the larger SU(3) symmetry. Consequently, the qualitative picture of the two-stage screening applies also for the Kanamori Hamiltonian.

We also performed the NRG simulations that confirm these weak-coupling RG findings. We calculated the dependence of spin and orbital Kondo temperatures for a range of parameters and electron occupancies. Except at very low values of the Hund's rule coupling strength, the spin Kondo temperature is significantly smaller (an order of magnitude or more). The smaller bare value of the spin-Kondo coupling as well as its slower running both contribute to such behavior.

The paper is structured as follows. In Sec. II we start with the description of the model. In Sec. III we present the Schrieffer-Wolff transformation, the resulting Kondo Hamiltonian, and the Kondo couplings. In Sec. III C we discuss the RG flow using the poor man's scaling approach. In Sec. IV we give the NRG results. In Sec. V we conclude with a discussion of the implications of our results and with prospects for future work. In Appendixes A and B we give technical details on the derivation of the Kondo Hamiltonian and RG flow, respectively. In Appendix C we compare the behavior of the Dworin-Narath and Kanamori models.

II. IMPURITY MODEL

The impurity model of interest to this paper reads

$$H_{\text{bath}} = \sum_{k,m,\sigma} \epsilon_k c^\dagger_{km\sigma} c_{km\sigma}, \tag{3}$$

$$H_{\text{hyb}} = \sum_{k,m,\sigma} V_k c^\dagger_{km\sigma} d_{m\sigma} + \text{H.c.} = V \sum_{m,\sigma} c^\dagger_{m\sigma} d_{m\sigma} + \text{H.c.}, \tag{4}$$

$$H_{\text{imp}} = -2J\mathbf{S}^2 - \alpha \frac{J}{2}\mathbf{L}^2 + \frac{U-3J}{2} N_d(N_d-1) + \epsilon_0 N_d, \tag{5}$$

with

$$N_d = \sum_{m,\sigma} d^\dagger_{m\sigma} d_{m\sigma},$$

$$\mathbf{S} = \sum_{m} d^\dagger_{m\sigma} \left(\frac{1}{2}\boldsymbol{\sigma}_{\sigma\sigma'}\right) d_{m\sigma'}, \tag{6}$$

$$\mathbf{L} = \sum_{\sigma} d^\dagger_{m\sigma} \mathcal{L}_{mm'} d_{m'\sigma}.$$

The operators $c^{(\dagger)}_{m\sigma}$ and $d^{(\dagger)}_{m\sigma}$ annihilate (create) bath and impurity electrons with spin $\sigma = \pm 1/2$ in orbital m; the orbital degeneracy is denoted as M. The noninteracting conduction electrons (H_{bath}) have energy ϵ_k, which corresponds to a flat density of states $\rho_0 = 1/2D_0$ with half-bandwidth D_0. In the hybridization function (H_{hyb}) we use the notation $\sum_k V_k c_{km\sigma} = V c_{m\sigma}$. The hybridization strength is defined as $\Gamma = \pi\rho_0 V^2$.

The interaction of the electrons on the impurity is described by the term H_{imp} where we introduced the parameter α that tunes the impurity interaction between the Dworin-Narath ($\alpha = 0$) and the Kanamori ($\alpha = 1$) case in a continuous way. We will refer to the impurity model above as the Anderson impurity model (AIM) to distinguish it from the Kondo model defined in the following. N_d is the total impurity charge operator, $\mathbf{S}$ is the total impurity spin operator ($\boldsymbol{\sigma}$ are Pauli matrices), and $\mathbf{L}$ is the total impurity orbital angular moment ($\mathcal{L}$ are spin-1 matrices for $M = 3$). The spin and orbital momentum operators obey the Lie algebra commutation relations and are normalized such that $\text{Tr}(X^\alpha X^\beta) = 2\delta_{\alpha,\beta}, X \in \{L, S\}$.

In the following section we derive an effective Kondo Hamiltonian for the simplest realistic model that captures the Hund's physics: the three orbital ($M = 3$) AIM with two electrons or holes occupying the impurity such that the ground state orbital moment and spin are $L = 1$, $S = 1$.

We set units such that $D_0 = 1$, $k_B = 1$, $g\mu_B = 1$.

III. KONDO HAMILTONIAN AND RG ANALYSIS

A. Schrieffer-Wolff transformation

To investigate the low-energy behavior of coupled bath and impurity electrons we derive an effective Kondo Hamiltonian in which the charge fluctuations on the impurity are suppressed. This is achieved using the canonical Schrieffer-Wolff transformation [28]. The interaction term that is induced by virtual fluctuations from the ground-state impurity multiplet into the high-energy manifolds with $n \pm 1$ electrons reads

$$H_{\text{K}} = -P_n H_{\text{hyb}} \left(\sum_a \frac{P^a_{n+1}}{\Delta E^a_{n+1}} + \sum_b \frac{P^b_{n-1}}{\Delta E^b_{n-1}} \right) H_{\text{hyb}} P_n. \tag{7}$$

Projector operators P_n project onto the atomic ground state multiplet with valence n. Projectors $P^a_{n\pm1}$ project onto the high energy multiplets having energy $E^a_{n\pm1}$ (indices a, b denote different invariant subspaces with respect to H_{imp}) and the virtual excitation energies are $\Delta E^a_{n\pm1} = E^a_{n\pm1} - E_n$ where E_n is the ground state energy; see Table I.

For the case of the Kanamori Hamiltonian, Eq. (7) can be rewritten (see Appendix A for the derivation) in the following "Kondo-Kanamori" form:

$$H_K = J_p N_f + J_s \mathbf{S}\cdot\mathbf{s} + J_l \mathbf{L}\cdot\mathbf{l} + J_q \mathbf{Q}\cdot\mathbf{q} + J_{ls}(\mathbf{L}\otimes\mathbf{S})\cdot(\mathbf{l}\otimes\mathbf{s}) + J_{qs}(\mathbf{Q}\otimes\mathbf{S})\cdot(\mathbf{q}\otimes\mathbf{s}). \tag{8}$$

N_f is the bulk electron charge operator at the position of the impurity, and $\mathbf{S}, \mathbf{L}, \mathbf{Q}$ ($\mathbf{s}, \mathbf{l}, \mathbf{q}$) are total impurity (bath) spin, orbit, and orbital quadrupole operators, respectively. The five

TABLE I. Excitation energies. The parameter b is defined in Eq. (12).

Index	N_d	L	S	ΔE
ΔE_1	1	1	1/2	$b(U-(4-\alpha)J)$
ΔE^a_3	3	0	3/2	$(1-b)(U-(4-\alpha)J)$
ΔE^b_3	3	2	1/2	$(1-b)U + J(b(4-\alpha)+2(1-\alpha))$
ΔE^c_3	3	1	1/2	$(1-b)U + J(b(4-\alpha)+2)$

(symmetric and traceless) quadrupole operators are second-order orbital tensor operators defined as

$$Q^{bc}_{i,j} = \frac{1}{2}\left(L^b_{i,m}L^c_{m,j} + L^c_{i,m}L^b_{m,j}\right) - \frac{2}{3}\delta_{b,c}\delta_{i,j}, \tag{9}$$

$$\mathrm{Tr}(Q^\alpha Q^\beta) = 2\delta_{\alpha,\beta}. \tag{10}$$

The Kondo Hamiltonian contains besides spin-spin, orbital-orbital, and quadrupole-quadrupole interaction also the mixed spin-orbital and spin-quadrupole products ($\mathbf{L}\otimes\mathbf{S}$,$\mathbf{Q}\otimes\mathbf{S}$, respectively). Equation (8) can be viewed as a multipole expansion of the exchange interaction for spin and orbital degrees of freedom; the highest orders (dipole for spin, quadrupole for orbital momentum) are related to the degrees of freedom carried by the particles ($\sigma = \pm 1/2$ for spin, $m = -1,0,1$ for orbital momentum).

For the Dworin-Narath Hamiltonian, the corresponding Kondo form reads

$$H_K^{\mathrm{DN}} = J_p N_f + J_s \mathbf{S}\cdot\mathbf{s} + J_t \mathbf{T}\cdot\mathbf{t} + J_{ts}(\mathbf{T}\otimes\mathbf{S})\cdot(\mathbf{t}\otimes\mathbf{s}). \tag{11}$$

In this expression, $\mathbf{s}$ is the total bath spin operator and $t^\alpha = \sum_{mm'\sigma} c^\dagger_{m\sigma}\tau^\alpha_{mm'}c_{m'\sigma}$, τ^α are the Gell-Mann matrices. $\mathbf{S}$ and $\mathbf{T}$ are the generators of spin-1 representation of SU(2) and the fundamental representation of SU(3), respectively.

The total set of eight generators $\{L,Q\}$ is, in fact, equivalent to the set of SU(3) generators $\{T\}$: Both sets constitute a basis for the traceless Hermitian 3×3 matrices. Reducing the SU(3) orbital symmetry to SO(3) symmetry leads to a splitting of the orbit-orbit and orbit-quadrupole coupling constants, i.e., $J_t \to J_l, J_q$ and $J_{ts} \to J_{ls}, J_{qs}$. One of the goals of this work is to study the consequences of this splitting.

B. Kondo coupling constants

We calculate the coupling constants for the ground-state multiplet with two electrons occupying the impurity ($N_d = 2$) that has angular momenta $L = 1, S = 1$. In the zero bandwidth limit, $V \to 0$, the impurity energy level which determines the impurity occupancy reads

$$\epsilon_0 = \frac{3+2\alpha}{2}J - (1+b)[U - J(4-\alpha)]. \tag{12}$$

It is measured from the Fermi level. The parameter $b \in [0,1]$ controls the occupancy of the impurity before the projection to the $N_d = 2$ subspace and determines the potential scattering term of the Kondo Hamiltonian. The term is written so that when $b \to 0$ and $b \to 1$ the atomic $N_d = 2$ ground state becomes degenerate with the atomic lowest states with occupancies $N_d = 1$ and $N_d = 3$, respectively. The excitation energies $\Delta E_{1,3}$ to states with impurity occupancy $N_d \pm 1 = 1,3$ are presented in Table I. Superscripts a,b,c denote the three multiplets with charge $N_d = 3$ having different values of spin and orbital moment.

We note in passing that under the particle-hole transformation [29] not only the potential scattering term but also the spin-orbital coupling and the quadrupole-quadrupole coupling terms of the Hamiltonian in Eq. (8) are odd. As a result, the twofold hypercharge degeneracy discussed in Ref. [30] does not apply even in the absence of potential scattering.

Next we calculate the Kondo coupling constants by comparing the matrix elements of Hamiltonians in Eqs. (7) and (8):

$$J_p = \frac{V^2}{18}\left(\frac{6}{\Delta E_1} - \frac{4}{\Delta E_3^a} - \frac{5}{\Delta E_3^b} - \frac{3}{\Delta E_3^c}\right), \tag{13}$$

$$J_s = \frac{V^2}{18}\left(\frac{6}{\Delta E_1} - \frac{2}{\Delta E_3^a} + \frac{5}{\Delta E_3^b} + \frac{3}{\Delta E_3^c}\right), \tag{14}$$

$$J_l = \frac{V^2}{12}\left(\frac{6}{\Delta E_1} + \frac{8}{\Delta E_3^a} - \frac{5}{\Delta E_3^b} + \frac{3}{\Delta E_3^c}\right), \tag{15}$$

$$J_q = \frac{V^2}{12}\left(\frac{6}{\Delta E_1} + \frac{8}{\Delta E_3^a} + \frac{1}{\Delta E_3^b} - \frac{3}{\Delta E_3^c}\right), \tag{16}$$

$$J_{ls} = \frac{V^2}{6}\left(\frac{6}{\Delta E_1} + \frac{4}{\Delta E_3^a} + \frac{5}{\Delta E_3^b} - \frac{3}{\Delta E_3^c}\right), \tag{17}$$

$$J_{qs} = \frac{V^2}{6}\left(\frac{6}{\Delta E_1} + \frac{4}{\Delta E_3^a} - \frac{1}{\Delta E_3^b} + \frac{3}{\Delta E_3^c}\right). \tag{18}$$

These bare Kondo couplings are presented in Fig. 1(a) for different values of the parameter b. The spin-spin coupling J_s is substantially smaller than others for most values of b and changes sign on approaching $b = 1$ that corresponds to the regime of valence fluctuations between $N_d = 2$ and $N_d = 3$ (at the degeneracy point between $N_d = 2$ and $N_d = 3$, the atomic average occupancy is $30/13 \approx 2.3$, while at the degeneracy point between $N_d = 2$ and $N_d = 1$, the atomic average occupancy is $8/5 = 1.6$). All couplings diverge on approaching the end points $b = 0$ and $b = 1$ where the cost for the charge excitations vanishes. The Kondo model and the derived couplings for the $N_d = 2$, $L = 1$, $S = 1$ atomic ground-state configuration cease to be valid there.

The results are qualitatively similar to those found for the Dworin-Narath model in Refs. [24,25] with the distinction that for the Kanamori Hamiltonian the orbital and quadrupole couplings are split:

$$J_q - J_l = \Delta J/2,$$
$$J_{qs} - J_{ls} = -\Delta J,$$

with

$$\Delta J = V^2\left(\frac{1}{\Delta E_3^c} - \frac{1}{\Delta E_3^b}\right) = \frac{2J\alpha V^2}{\Delta E_3^b \Delta E_3^c}.$$

This results from the different energies of the $L = 1$ and $L = 2$ three-electron spin-doublet multiplets, caused by the $-\alpha(J/2)\mathbf{L}^2$ term in the Hamiltonian. For the Kanamori model with $\alpha = 1$ the splitting is largest when the Hund's coupling reaches

$$J = \frac{(1-b)U}{\sqrt{9b^2+6b}}. \tag{19}$$

For two electrons at the impurity ($b \approx 1/2$) this occurs for $J = 0.22U$. Figure 1(b) shows how the splitting develops as the Hund's coupling J is increased from zero, while keeping the parameter that controls the charge fluctuations, $U_{\mathrm{eff}} = U - 3J$, constant. In other words, as J is varied, the Hubbard repulsion U is adjusted so that the effective impurity repulsion $U_{\mathrm{eff}} = E(3) + E(1) - 2E(2) = U - 3J$ is kept fixed; here $E(N)$ denotes the energy of the lowest multiplet with occupancy N. The splittings of Kondo couplings are initially linear in J, but then slowly fall off as $1/J$. For

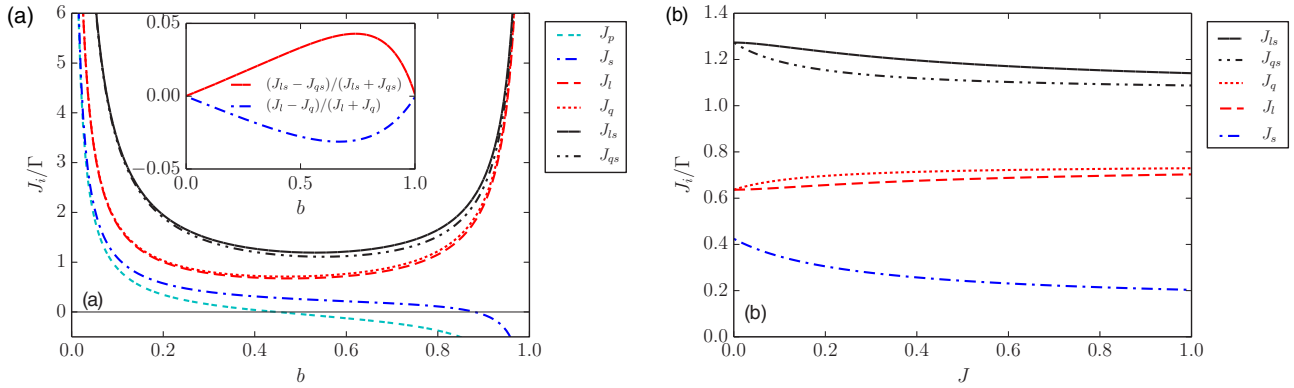

FIG. 1. (a) Bare Kondo exchange coupling constants of the effective Kondo-Kanamori model as a function of the impurity level parameter b. Model parameters are $U = 3.2, J = 0.4$. The inset shows the relative size of the splittings through ratios $(J_l - J_q)/(J_l + J_q)$ and $(J_{ls} - J_{qs})/(J_{ls} + J_{qs})$. (b) Bare Kondo couplings as a function of Hund's coupling J for constant $U_{\text{eff}} = U - 3J = 2, b = 0.5$.

any J, the hierarchy of coupling constants is $J_s < J_l \lesssim J_q < J_{qs} \lesssim J_{ls}$.

For $\alpha = 0$, the $n = 3$ excited states with spin $S = 1/2$ and orbital moment $L = 1, L = 2$ become degenerate and the following relation holds $\Delta E_3^b = \Delta E_3^c = \Delta E_3^a + 6J = \Delta E_3 + 6J$, and we find

$$J_p = \frac{V^2}{9}\left(\frac{3}{\Delta E_1} - \frac{2}{\Delta E_3} - \frac{4}{\Delta E_3 + 6J}\right), \quad (20)$$

$$J_s = \frac{V^2}{9}\left(\frac{3}{\Delta E_1} - \frac{1}{\Delta E_3} + \frac{4}{\Delta E_3 + 6J}\right), \quad (21)$$

$$J_l = J_q = \frac{V^2}{6}\left(\frac{3}{\Delta E_1} + \frac{4}{\Delta E_3} - \frac{1}{\Delta E_3 + 6J}\right), \quad (22)$$

$$J_{ls} = J_{qs} = \frac{V^2}{3}\left(\frac{3}{\Delta E_1} + \frac{2}{\Delta E_3} + \frac{1}{\Delta E_3 + 6J}\right). \quad (23)$$

The results of Ref. [25] are recovered if one omits terms proportional to $(\Delta E_3 + 6J)^{-1}$ that come from the transitions to $n = 3, S = 1/2$ states neglected there and rescales the coupling constants by a factor of 2 due to the different definition of the Hamiltonian.

C. Poor man's scaling analysis

We now discuss the low-energy physics of the derived Kondo-Kanamori Hamiltonian within the weak-coupling RG approach [31]. The scaling functions $\beta_i = dJ_i/d\ln(D)$ describe the renormalization of the coupling constants as the half-bandwidth D is progressively reduced. For $S = 1$, $L = 1$ impurity configuration, corresponding to the ground-state multiplet for two electrons the scaling functions to the lowest

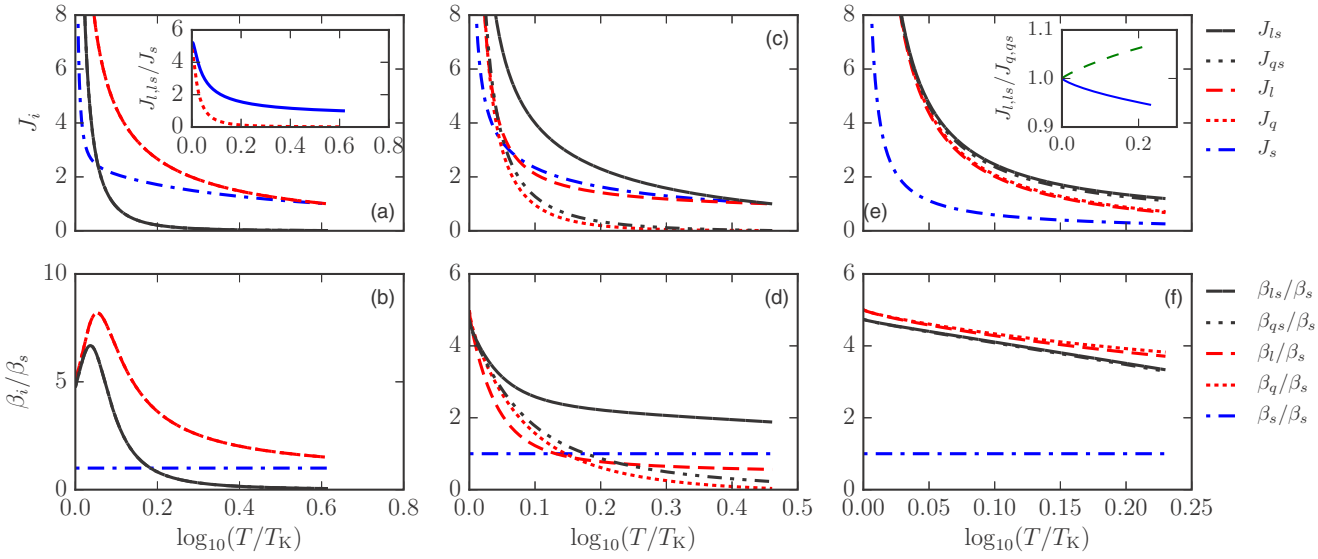

FIG. 2. Scaling of the Kondo coupling constants (top) and β divided by the spin scaling function β_s (bottom) for different initial couplings. The horizonal scale is such that the origin corresponds to $T = T_K$, where the coupling constants diverge. In (a) and (b) the mixed bare couplings are suppressed, $J_{ls} = J_{qs} = J_s/100$, where $J_s = J_l = J_q = 1$. In the inset in (a) we plot ratios J_l/J_s (solid line) and J_{ls}/J_s (dotted line). In (c) and (d) the quadrupole couplings are suppressed, $J_{q,qs} = J_s/100$ and $J_s = J_l = J_{ls} = 1$. In (e) and (f) we use the bare couplings that correspond to the Anderson impurity model with parameters $U = 3.2, J = 0.4, \Gamma = 1$. Inset in (f) shows ratio between the orbital and quadrupole couplings. Solid and dashed lines correspond to ratios J_l/J_q and J_{ls}/J_{qs}, respectively.

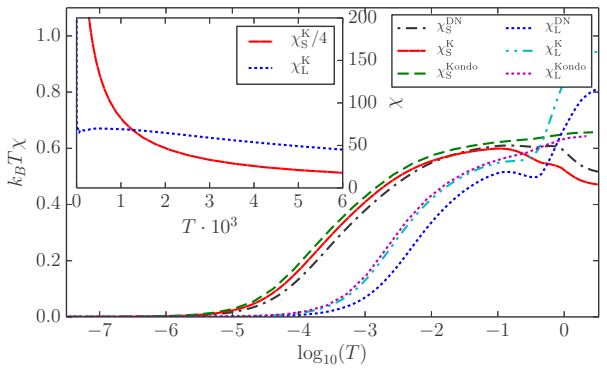

FIG. 3. The NRG results for the effective moments $\chi_{S,L}T$ (main panel) and susceptibility $\chi_{S,L}$ (inset) as a function of temperature for Dworin-Narath, Kanamori, and Kondo-Kanamori models. $U = 3.2, J = 0.4, \Gamma = 0.1$.

order read

$$\beta_p = 0, \tag{24}$$

$$\beta_s = -\frac{1}{9}\left(3{J_{ls}}^2 + 5{J_{qs}}^2 + 9{J_s}^2\right), \tag{25}$$

$$\beta_l = -\frac{1}{4}\left({J_l}^2 + 2{J_{ls}}^2 + 5\left({J_q}^2 + 2{J_{qs}}^2\right)\right), \tag{26}$$

$$\beta_q = -\frac{3}{2}(J_l J_q + 2J_{ls} J_{qs}), \tag{27}$$

$$\beta_{ls} = -\frac{1}{6}(3J_l J_{ls} + 5J_{ls} J_{qs} + 12J_{ls} J_s + 15J_q J_{qs}), \tag{28}$$

$$\beta_{qs} = -\frac{1}{12}(J_{qs}(18J_l + 7J_{qs} + 24J_s) + 3{J_{ls}}^2 + 18J_{ls} J_q). \tag{29}$$

For a particle-hole symmetric band (as is the case for the flat density of states, $\rho_0 = 1/2$, used here) the potential scattering operator is marginal, $\beta_p = 0$.

The symmetry of the Hamiltonian is reflected in the scaling equations. For instance, for vanishing Hund's orbital coupling in the AIM, the initial orbital and quadrupole coupling constants in Eq. (13) are equal $J_q = J_l$ and $J_{qs} = J_{ls}$. For such SU(3) orbitally symmetric choice of bare coupling constants, the respective scaling functions coincide: $\beta_q = \beta_l, \beta_{qs} = \beta_{ls}$ and hence $J_q = J_l$ and $J_{qs} = J_{ls}$ also after RG scaling.

It is interesting to omit the cross-terms by setting $J_{ls} = J_{qs} = 0$, which is preserved also after RG flow. Hence, the spin and orbit coupling constants undergo a separate scaling in this case. From the ratio of the two scaling functions $\beta_l/\beta_s = (3/2)J_l^2/J_s^2$ one sees that besides the larger bare value of J_l additional factor 3/2 (the ratio of the orbital and spin degeneracy) helps the faster renormalization of orbital couplings. This behavior, associated with the larger SU(3) symmetry holds in the case of $J_q = J_l$.

We numerically solved the scaling equations for three characteristic cases; see Fig. 2. The top panels show the Kondo couplings and the bottom panels the scaling functions β divided by the spin scaling function β_s.

In the first case, see the left-most panels, Figs. 2(a) and 2(b), we set the initial values to unity $J_s = J_l = J_q = 1$, but we suppressed the cross-terms and set $J_{ls} = J_{qs} = 1/100$. The orbital coupling renormalizes to strong coupling faster than the orbital coupling. The mixed-spin orbital coupling J_{ls} also increases faster, and exceeds the values of J_s at low temperatures.

The second case, shown in the middle panels, Figs. 2(c) and 2(d), demonstrates the effects of the splitting between the orbit and quadrupole terms. We set the initial values to unity $J_s = J_l = J_{ls} = 1$ for all but the quadrupole and

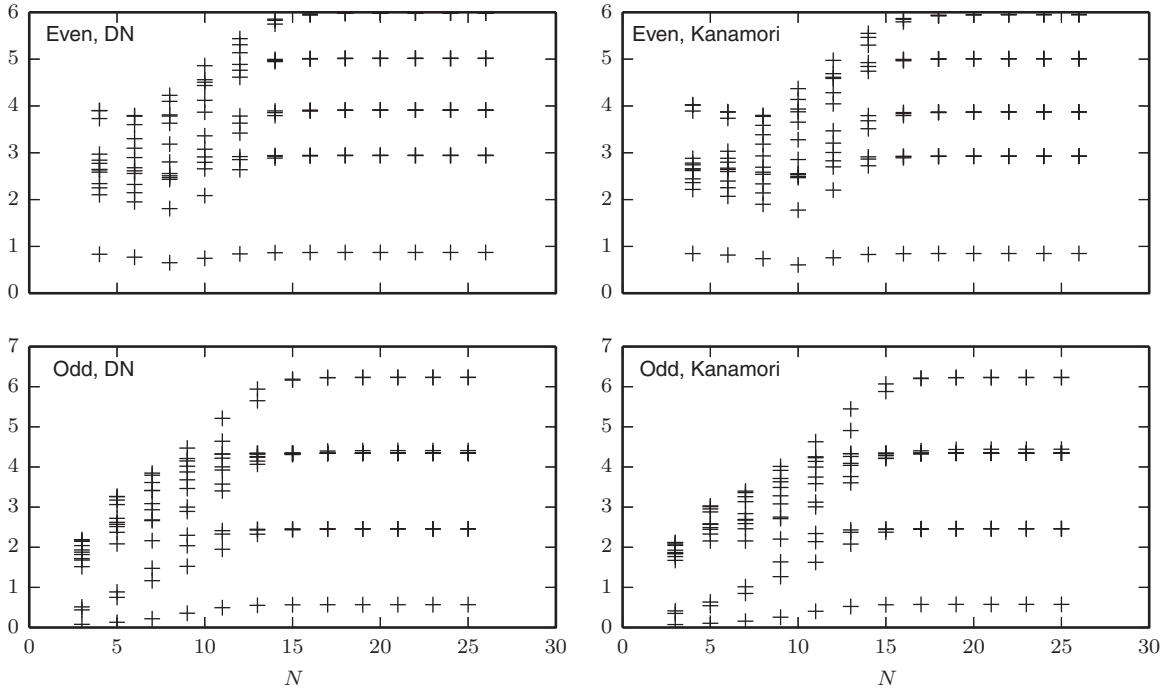

FIG. 4. NRG finite size spectra for the DN and Kanamori interaction. Parameters are $U = 3.2$, $J = 0.4$, $N_d = 2$.

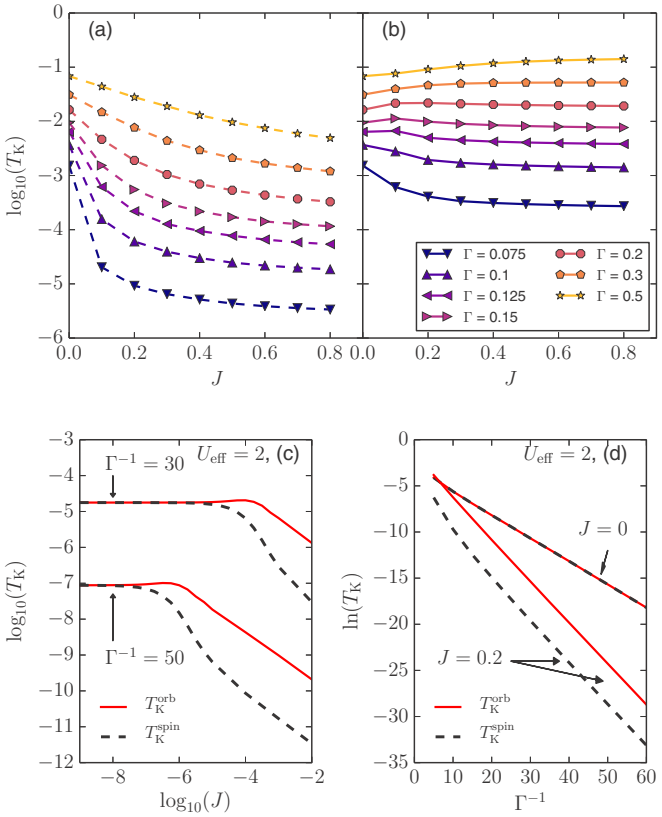

FIG. 5. Kondo temperatures for the Kanamori model at fixed $U_{\rm eff} = 2$ and fixed impurity occupancy $N_d = 2$. (a) Spin and (b) orbit Kondo temperatures as a function of the Hund's coupling J for different values of hybridization Γ. (c) Spin and orbit Kondo temperatures plotted versus logarithm of the Hund's coupling J. (d) Spin and orbit Kondo temperatures as a function of Γ^{-1} for two values of $J = 0, J = 0.2$.

spin-quadrupole coupling constants that we suppressed: $J_q = J_l/100, J_{qs} = J_{ls}/100$. When the quadrupole terms are small they can be neglected in the scaling equations [Eqs. (25)–(29)]. In this case initially the scaling of the spin coupling is faster than the scaling of the orbit coupling, because the normally large contribution of the quadrupole terms $J_{q,qs}$ to β_l is not present. Only when $J_{q,qs}$ become comparable to $J_{l,ls}$, the renormalization of the orbital coupling becomes faster than the renormalization of the spin coupling. It is important to note that the splitting between the orbit and quadrupole and spin-orbit and spin-quadrupole terms disappears at low energies.

The case of realistic set of initial coupling constants corresponding to the Anderson model (with parameters $U = 3.2, J = 0.4, \Gamma = 1$) is displayed in Figs. 2(e) and 2(f). One sees that the splitting between the orbital and quadrupole terms, which is weak already initially, completely disappears on approaching the low energies [best seen in inset to Fig. 2(e) that displays the ratio of the two]. Thus the multiplet splitting due to orbital interaction in the Anderson model becomes insignificant at low energies. The SU(3) and SO(3) symmetric models describe the same low-energy physics. Similar dynamical symmetry generation (or restoration) has been observed in a number of other quantum impurity models as well [32–36].

IV. NUMERICAL RENORMALIZATION GROUP RESULTS

Using the NRG technique [37] we solve the Kanamori, Dworin-Narath (DN), and the Kondo impurity model. The NRG results validate the qualitative insights from the poor man's scaling approach discussed above. The two-stage screening behavior with the spin being screened at a temperature that is significantly lower than that for the orbital moment occurs in all three models.

We have implemented an NRG code with conserved quantum numbers (Q,S,L), corresponding to total charge, total spin and total orbital angular momentum, i.e., using the U(1)⊗SU(2)⊗SO(3) symmetry. This allows one to perform three-orbital calculations even with modest computation resources.

A. Comparison between Dworin-Narath, Kanamori, and Kondo-Kanamori results

In Fig. 3 we present the temperature dependence of the effective spin and orbital moments, $\chi_S T$ and $\chi_L T$, where $\chi_{L,S}$ are the impurity orbital and spin susceptibilities. The Kanamori results are compared to those for the Kondo model with exchange couplings set by Eqs. (24)–(29) and those for the more symmetric Dworin-Narath model. At high temperatures, the results for different models significantly differ due to different high-energy physics. Nevertheless, at lower temperatures the different models behave alike. In particular, the Kondo-Kanamori curves are close to the Kanamori ones (the differences become even smaller if the ratio of the interaction to the hybridization is diminished) which validates our analytical approach. The Dworin-Narath model behaves qualitatively the same, the main distinction being noticeably higher screening temperature of the orbital moments.

In the inset to Fig. 3 we present the spin and orbital susceptibilities. The former is scaled by $1/4$ for easier comparison. The spin susceptibility is much larger than the orbital susceptibility and the latter saturates at higher temperatures. This again shows faster screening of the orbital degrees of freedom. The orbital susceptibility has a weak maximum before saturating to the low-temperature value. Similar behavior was found in earlier work [24].

To confirm the asymptotic equivalence of the models, we present in Fig. 4 the finite size spectra calculated with NRG for the DN and the Kanamori impurity models as a function of the NRG step. The two spectra are the same at low energies, which shows that the two models have exactly the same low-energy Fermi-liquid fixed point with excitation spectrum parametrized by the quasiparticle phase shift which is determined by the Friedel sum rule for fixed occupancy $N_d = 2$.

B. Kanamori results at integer occupancy $N_d = 2$

We now discuss the Kanamori model in more detail. It is convenient to define the spin and orbital Kondo temperatures as the scale at which the respective effective moment diminishes below a constant. We take the constant to be 0.07 for spin and $0.07l(l+1)/s(s+1)$ for the orbital effective moment [10]. l,s are the orbital moment and the spin of electrons, i.e., $l = 1$, $s = 1/2$, hence $l(l+1)/s(s+1) = 8/3$. It is of interest to

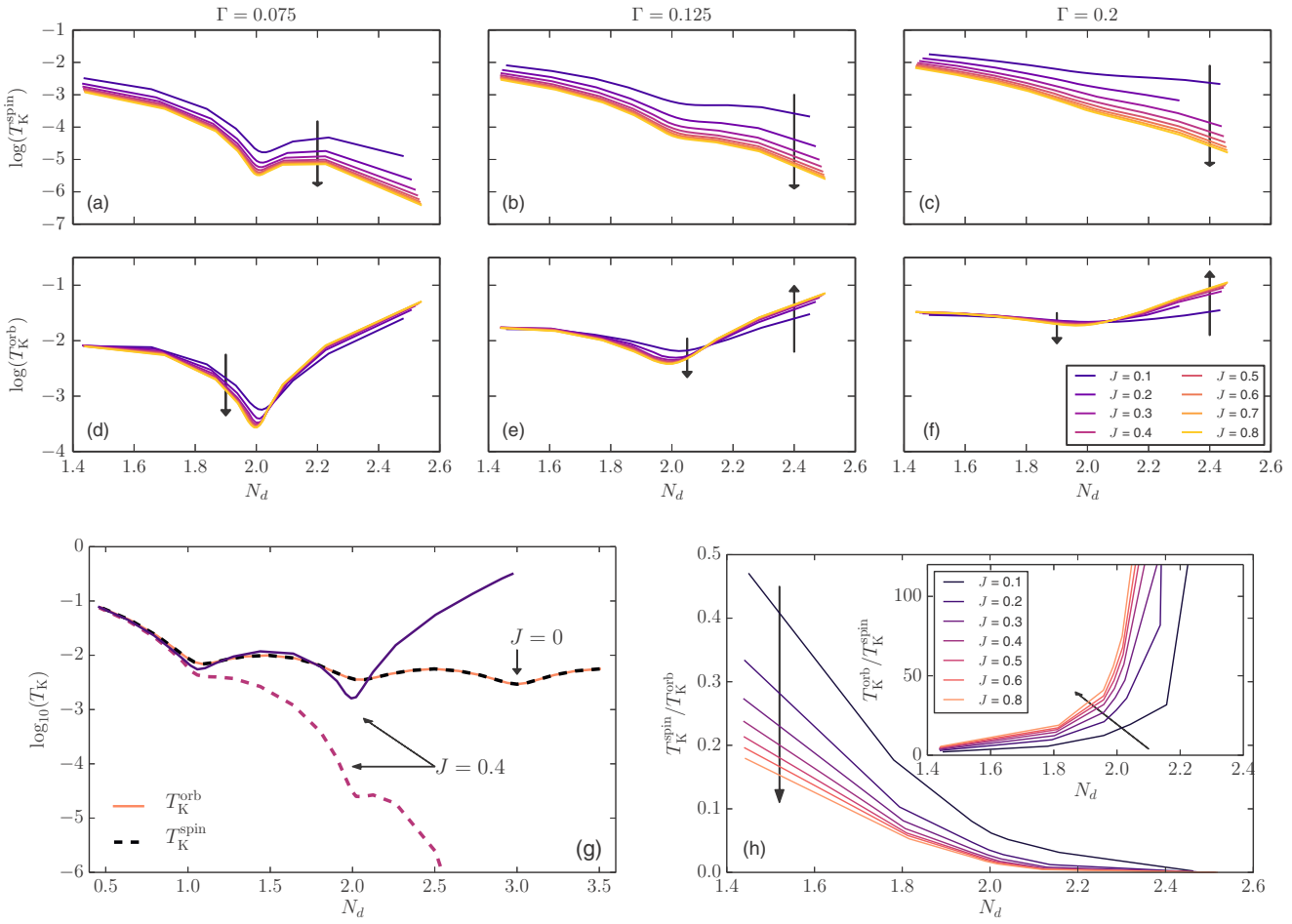

FIG. 6. Kanamori model. (a)–(f) Spin and orbit Kondo temperatures as a function of the impurity occupancy N_d for different values of the Hund's coupling J at fixed $U_{\rm eff} = 2$. (g) Spin and orbit Kondo temperatures in a larger region of impurity filling for zero and nonzero Hund's coupling. At $J = 0$ the spin and orbit Kondo temperature are equal. $\Gamma = 0.1$. (h) Ratio between the spin and orbit Kondo temperatures. The arrows indicate the direction of increasing J. The inset shows the inverse ratios.

know how the spin $T_K^{\rm spin}$ and orbital $T_K^{\rm orb}$ Kondo temperatures vary with the parameters of the Hamiltonian. We first discuss the results at an integer occupancy $N_d = 2$.

In Figs. 5(a)–5(c) we plot $T_K^{\rm spin}$ and $T_K^{\rm orb}$ as a function of the Hund's rule coupling J for several hybridization strengths Γ. When J is smaller than the Kondo scale of the $J = 0$ model, $T_{\rm K}(J = 0) = T_{\rm K}^0$, the moments are screened before the Hund's coupling has effect. In this regime symmetry of the model becomes SU(M × N), hence only a single Kondo scale exists and $T_K^{\rm spin} = T_K^{\rm orb}$. The Kondo temperature dependence on J is initially slow, but becomes faster when J becomes larger than $T_{\rm K}^0$ as seen from Fig. 5(c). In addition, close to the $J \sim T_{\rm K}^0$ point, $T_K^{\rm spin}$ becomes smaller than $T_K^{\rm orb}$. Unlike $T_K^{\rm spin}$ that decreases monotonously with J, $T_K^{\rm orb}$ has a weak maximum at J above $T_K(J = 0)$, which arises as a consequence of an interplay between the orbital, quadrupole, and spin-orbital, spin-quadrupole interactions. This can be understood from the behavior of the coupling constants at small J. Namely, upon expanding the Kondo couplings to first order in J one sees that the orbital-orbital and quadrupole-quadrupole Kondo interactions increase with J, e.g., $J_l = J_l^0 + \alpha J$, while the other coupling constants decrease, e.g., $J_{ls} = J_{ls}^0 - \beta J$, where α, β are positive constants.

It is interesting to look at the spin and orbit Kondo temperatures also as a function of hybridization. In Fig. 5(d) we present the logarithms of $T_K^{\rm spin}$ and $T_K^{\rm orb}$ as a function of Γ^{-1} for zero and nonzero value of Hund's rule coupling. In the first case, the spin and orbit Kondo scales are the same for all Γ. Conversely, in the second case, the spin Kondo temperature is below the orbit Kondo temperature for all Γ. The leading exponential dependence on Γ is the same for both $T_K^{\rm spin}$ and $T_K^{\rm orb}$, as seen from equal slopes of the lines. The slopes depend on the repulsion and are $-U_{\rm eff}/c$ with (at $N_d = 2$) $c \approx 3$ for the zero-J case and $c \approx 4$ for the finite-J case. The difference is due to the increased degeneracy of multiplets in the $J = 0$ case.

C. Kanamori results away from integer filling

We now turn to the results away from integer filling. In Figs. 6(a)–6(f) we display the Kondo temperatures for several Γ and J, still keeping $U_{\rm eff} = 2$ fixed, as a function of the impurity occupancy N_d in an interval around 2. The spin and orbital Kondo temperatures behave differently. $T_K^{\rm spin}$ exhibit an overall diminishing trend as N_d is increased towards half-filling ($N_d = 3$) with a shallow minimum at $N_d = 2$

that becomes less pronounced for larger Γ where $\log T_K^{\rm spin}$ is roughly linear in N_d. Conversely, $T_K^{\rm orb}$ increases when occupancy is changed from $N_d = 2$ in both directions for all values of Γ.

The different behavior of both Kondo temperatures on approaching half-filling is due to the lowest states at $N_d = 3$ having large spin but vanishing orbital moment, $L = 0, S = 3/2$, thus the screening of the spin is strongly suppressed because of its large size [14,21], while the orbital moment is screened at a higher temperature. At half-filling, the notion of orbital Kondo temperature becomes meaningless, as the orbital moment is zero also in the limit of vanishing hybridization. This distinction disappears for $J = 0$; see Fig. 6(g) where the results for zero and nonzero J are shown in a broader range of N_d. For $J = 0$, the spin and orbit Kondo temperatures are the same.

On approaching small occupancies, $N_d \lesssim 1$, the Kondo temperatures rapidly increase and no distinction is seen between zero and nonzero J cases in Fig. 6(g). When there is on average a single electron in the impurity the Hund's coupling has no effect.

In Fig. 6(h) the ratio between the spin and orbital Kondo temperatures is shown. One sees that $T_K^{\rm orb}/T_K^{\rm spin}$ rapidly increases as N_d is increased and at the occupancy $N_d = 2$ this ratio is about 10 and is further increasing as we approach half-filling.

V. CONCLUSION

We investigated the low-energy behavior of the Kanamori model in the RG and NRG approaches. We derived the appropriate Kondo model that is described in terms of spin, orbital, and quadrupole degrees of freedom. At the lowest energies the splitting between the orbital and quadrupole coupling constants becomes insignificant, therefore similar behavior as for a Hamiltonian with a larger SU(3) [25] symmetry can be expected. The NRG results confirm these poor-man's scaling findings. In particular, both models have the same strong-coupling Fermi-liquid stable fixed point at low energies and approach this fixed point in a similar way (in the physically relevant parameter range). We calculated the dependence of the spin and orbital Kondo temperatures on interaction parameters, hybridization, and impurity occupancy. The orbital Kondo temperature is higher, thus orbital moments are quenched first as the temperature is lowered. This behavior starts to occur as soon as the Hund's rule coupling is increased above the Kondo temperature of the problem without the Hund's rule coupling. The screening of the spin moments occurs at a temperature that is about an order of magnitude smaller [38]. The ratio of the orbital Kondo temperature to the spin Kondo temperature becomes particularly large as the impurity occupancy is increased towards half-filling. Our results demonstrate that the NRG is capable of treating problems with realistic three-orbital interactions. This method could hence be used in the DMFT calculations, too. Another interesting line of investigation is the analysis of the derived Kondo impurity model for parameters that do not correspond to the Anderson-type model. Our preliminary results reveal a rich phase diagram with several distinct non-Fermi-liquid phases.

ACKNOWLEDGMENTS

We acknowledge the support of the Slovenian Research Agency (ARRS) under Grants No. P1-0044 and No. J1-7259.

APPENDIX A: KONDO HAMILTONIAN DERIVATION

In this appendix we perform the Schrieffer-Wolff transformation to derive the Kondo Hamiltonian from the AIM with either the Dworin-Narath or Kanamori interaction. The Kondo Hamiltonian having SO(3) orbital and SU(2) spin symmetry was earlier written in terms of unit tensor operators in Ref. [39]. The Kondo Hamiltonian having SU(M) orbital and SU(N) spin symmetry was derived in Ref. [25].

The Schrieffer-Wolff transformation reads

$$H_{\rm K} = -P_n H_{\rm hyb}\left(\sum_a \frac{P^a_{n+1}}{\Delta E^a_{n+1}} + \sum_b \frac{P^b_{n-1}}{\Delta E^b_{n-1}}\right) H_{\rm hyb} P_n. \quad \text{(A1)}$$

The projector operator P_n projects onto the atomic ground-state multiplet with occupancy n. The projectors $P^a_{n\pm1}$ project onto the high-energy atomic multiplets having energy $E^a_{n\pm1}$ (indices a,b denote the different invariant subspaces with respect to $H_{\rm imp}$ as presented in the main text) and the virtual excitation energies are $\Delta E^a_{n\pm1} = E^a_{n\pm1} - E_n$, E_n being the ground-state energy.

We adopt the Einstein summation notation and for the sake of clarity we at first disregard all the constants (e.g., $V^2/\Delta E$). The projection operators to atomic multiplets transform as an identical representation under all symmetry transformations of the problem, hence the multiplet splitting of the excited states affects only the coupling constants (we write $\Gamma = H_{\rm hyb}$):

$$\sum_a \langle n|\Gamma \frac{P^a_{n+1}}{\Delta E^a_{n+1}} \Gamma|n\rangle = \sum_a \frac{1}{\Delta E^a_{n+1}} \langle n|\Gamma\Gamma|n\rangle. \quad \text{(A2)}$$

$|n\rangle = P_n|\Psi_{LS}\rangle$ is the ground state with valence n, orbital moment L, and spin S. The virtual charge excitation process conserves the impurity charge, thus $P_n d^\dagger_j d^\dagger_i P_n = 0$. The nonzero terms in the Kondo Hamiltonian are of the form,

$$H'_K = P_n\Gamma\Gamma P_n = P_n(c^\dagger_{i\sigma_i} d_{i\sigma_i} d^\dagger_{k\sigma_k} c_{k\sigma_k} + \text{H.c.})P_n, \quad \text{(A3)}$$

Next we insert an identity,

$$c^\dagger_{i\sigma_i} d_{i\sigma_i} d^\dagger_{k\sigma_k} c_{k\sigma_k} = (c^\dagger_{i\sigma_i}\delta_{i,l}\delta_{\sigma_i,\sigma_l} d_{l\sigma_l})(d^\dagger_{k\sigma_k}\delta_{k,j}\delta_{\sigma_k,\sigma_j} c_{j\sigma_j}), \quad \text{(A4)}$$

and use the following group-theoretical relations [40,41]:

$$\delta_{i,l}\delta_{k,j} = \frac{1}{m}\delta_{i,j}\delta_{k,l} + \frac{1}{a}(\tau^b)_{i,j}(\tau^b)_{k,l},\ \text{SU}(m), \quad \text{(A5)}$$

$$\delta_{i,l}\delta_{k,j} = \delta_{i,k}\delta_{j,l} + \frac{2}{a}(T^b)_{i,j}(T^b)_{k,l},\ \text{SO}(m). \quad \text{(A6)}$$

The generators τ, T live in the defining (fundamental) representation of the SU(m), SO(m) symmetric Lie group, respectively. The constant a depends on the normalization of the generators $\text{Tr}(T^b T^c) = a\delta_{b,c}$ (typically $a = 2$). In the SU(2) case τ are the Pauli matrices and in the SU(3) case τ are the Gell-Mann matrices.

To obtain the Kondo Hamiltonian from the AIM with the Dworin-Narath interaction in terms of spin and orbital operators, we insert the identity (A5) into Eq. (A4) for the spin and orbital degrees of freedom (since both have SU symmetry).

The relation (A5) leads to a result in which the dummy indices associated with the bulk operators $c_{i,j}$ are independent from the indices associated with the impurity operators, and can be summed over to yield spin/orbital momentum operators. The Kondo Hamiltonian with the Dworin-Narath interaction reads

$$H_K^{\mathrm{DN}} = J_p N_f + J_s \mathbf{S}\cdot\mathbf{s} + J_t \mathbf{T}\cdot\mathbf{t} + J_{ts}(\mathbf{T}\otimes\mathbf{S})\cdot(\mathbf{t}\otimes\mathbf{s}). \tag{A7}$$

Bath operators are defined as

$$\mathbf{s} = \sum_m c^\dagger_{m\sigma}\boldsymbol{\sigma}_{\sigma\sigma'}c_{m\sigma'}, \qquad \mathbf{t} = \sum_\sigma c^\dagger_{m\sigma}\boldsymbol{\tau}_{mm'}c_{m'\sigma}. \tag{A8}$$

$\boldsymbol{\tau}$,$\boldsymbol{\sigma}$ are the Pauli and Gell-Mann matrices, respectively. $\mathbf{S}$ and $\mathbf{T}$ are the generators of spin-1 representation of SU(2) and the fundamental representation of SU(3).

On the other hand the relation (A6) does not decouple the bulk/impurity dummy indices due to the term $\delta_{i,k}\delta_{j,l}$. However, this problematic term can be, for the three-dimensional SO(3) symmetric group, rewritten as

$$\delta_{i,l}\delta_{k,j} = \frac{1}{3}\delta_{i,j}\delta_{k,l} + \frac{1}{2}T^c_{i,j}T^c_{k,l} + \frac{1}{2}Q^{de}_{i,j}Q^{de}_{k,l}, \tag{A9}$$

which does lead to the desired decoupling. Above we used the orbital quadrupole operators defined as

$$Q^{bc}_{i,j} = \frac{1}{2}\left(T^b_{i,m}T^c_{m,j} + T^c_{i,m}T^b_{m,j}\right) - \frac{2}{3}\delta_{b,c}\delta_{i,j}, \tag{A10}$$

$$\mathrm{Tr}(Q^\alpha Q^\beta) = 2\delta_{\alpha,\beta}, \tag{A11}$$

which are symmetric and traceless. We derive the identity (A9) by calculating $\sum_{b,c} Q^{bc}_{ij}Q^{bc}_{kl}$ and using the identity (A6). By inserting the identity (A9) for orbital and (A5) for spin degrees of freedom into the Hamiltonian (A4), we express the Kondo Kanamori Hamiltonian as

$$H_K = J_p N_f + J_s \mathbf{S}\cdot\mathbf{s} + J_l \mathbf{L}\cdot\mathbf{l} + J_q \mathbf{Q}\cdot\mathbf{q} + J_{ls}(\mathbf{L}\otimes\mathbf{S})\cdot(\mathbf{l}\otimes\mathbf{s}) + J_{qs}(\mathbf{Q}\otimes\mathbf{S})\cdot(\mathbf{q}\otimes\mathbf{s}). \tag{A12}$$

$\mathbf{S}$,$\mathbf{L}$,$\mathbf{Q}$ ($\mathbf{s}$,$\mathbf{l}$,$\mathbf{q}$) are total impurity (bath) spin, orbit, orbital-quadrupole operators, respectively [42].

APPENDIX B: RG FLOW

In the second order of the perturbation theory we integrate out the scattering events to the states close to the band edges, $\pm\epsilon \in [D-\delta D, D]$. The correction to the renormalized Kondo interaction is

$$\Delta H_{\mathrm{K}} \approx \frac{1}{\Delta E} H_K P H_K. \tag{B1}$$

The projector P describes all the scattering events of electrons from the impurity to the band edges. The prefactor is $1/\Delta E = \rho|\delta D|(E - D + \epsilon_k)^{-1} \approx \rho|\delta D|D^{-1}$. We assume that the conduction band is wide. D is the half-bandwidth, E is the energy measured relative to the ground state of the conduction electron gas and can be neglected, and ϵ_k is the energy of electrons near the Fermi surface and can also be neglected relative to D.

In the following we present a convenient way for calculating the second-order corrections to the renormalized Hamiltonian using the completeness relations from the previous section. We will illustrate the procedure on the case of the spin-spin Kondo interaction term $J\mathbf{S}\cdot\boldsymbol{\sigma}$ for a single orbital model with $S = 1/2$. First, we write the impurity operators in terms of the fermionic operators,

$$S^\alpha \to d^\dagger_i \sigma^\alpha_{ij} d_j, \tag{B2}$$

with additional constraint $d^\dagger_\uparrow d_\uparrow + d^\dagger_\downarrow d_\downarrow = 1$. $d^\dagger_i$,d_i creates/annihilates an electron on the impurity with spin $i \in \{\uparrow,\downarrow\}$, and σ^α are the Pauli matrices. The bulk electron spin operator is

$$\sigma^\alpha \to c^\dagger_i \sigma^\alpha_{ij} c_j, \tag{B3}$$

and $c^\dagger_i$,c_i creates/annihilates an electron with spin i in the bulk. The spin-spin operators may be expressed in terms of Kronecker δ symbols using the following completeness relation:

$$\sum_\alpha (\sigma^\alpha)_{i,j}(\sigma^\alpha)_{k,l} = 2\delta_{i,l}\delta_{k,j} - \delta_{i,j}\delta_{k,l}. \tag{B4}$$

[For other operators, such as orbital, quadrupole, and mixed operators, one can derive similar expressions from Eqs. (A5), (A6), and (A10).] After inserting the completeness relation we obtain

$$J^2 \sum_{ijkl}(2\delta_{i,l}\delta_{k,j} - \delta_{i,j}\delta_{k,l}) d^\dagger_i d_j c^\dagger_k c_l P \times \sum_{mnop}(2\delta_{m,p}\delta_{o,n} - \delta_{m,n}\delta_{o,p}) d^\dagger_m d_n c^\dagger_o c_p \tag{B5}$$

$$= J^2 \sum_{ijkl}\sum_{mnop} A^{ijkl}_{mnop} P d^\dagger_i d_j d^\dagger_m d_n c^\dagger_k c_l c^\dagger_o c_p. \tag{B6}$$

The projector P consists of two contributions:

$$P = \delta_{jm}(\delta_{lo} + \delta_{kp}). \tag{B7}$$

The first term δ_{jm} follows from the single-occupancy constraint of auxiliary fermions, while the second term $\delta_{lo} + \delta_{kp}$ describes the processes that involve scattering of electrons/holes to the upper/lower band edge. In the expressions one can use $c^\dagger_{\sigma k}c_{\sigma k} = 0$ for the electron states k in the upper band edge that are assumed empty and $c^\dagger_{\sigma k}c_{\sigma k} = 1$ for the electron states k at the lower band edge that are assumed filled.

Now we sum over the indices m,o to eliminate Kronecker δ symbols that come from the projection operator. The contribution of the electron scattering to the upper band edge reads

$$J^2 \sum_{ijkl}\sum_{np} A^{ijkl}_{jnlp} d^\dagger_i d_n c^\dagger_k c_p. \tag{B8}$$

Next we sum over the dummy indices j,l. The correction to the Kondo exchange reads

$$J^2 \sum_{iknp}(-4\delta_{ip}\delta_{kn} + 5\delta_{in}\delta_{kp}) d^\dagger_i d_n c^\dagger_k c_p \tag{B9}$$

$$= -2J^2 \mathbf{S}\cdot\boldsymbol{\sigma} + 3J^2 \sum_{iknp}\delta_{in}\delta_{kp} d^\dagger_i d_n c^\dagger_k c_p. \tag{B10}$$

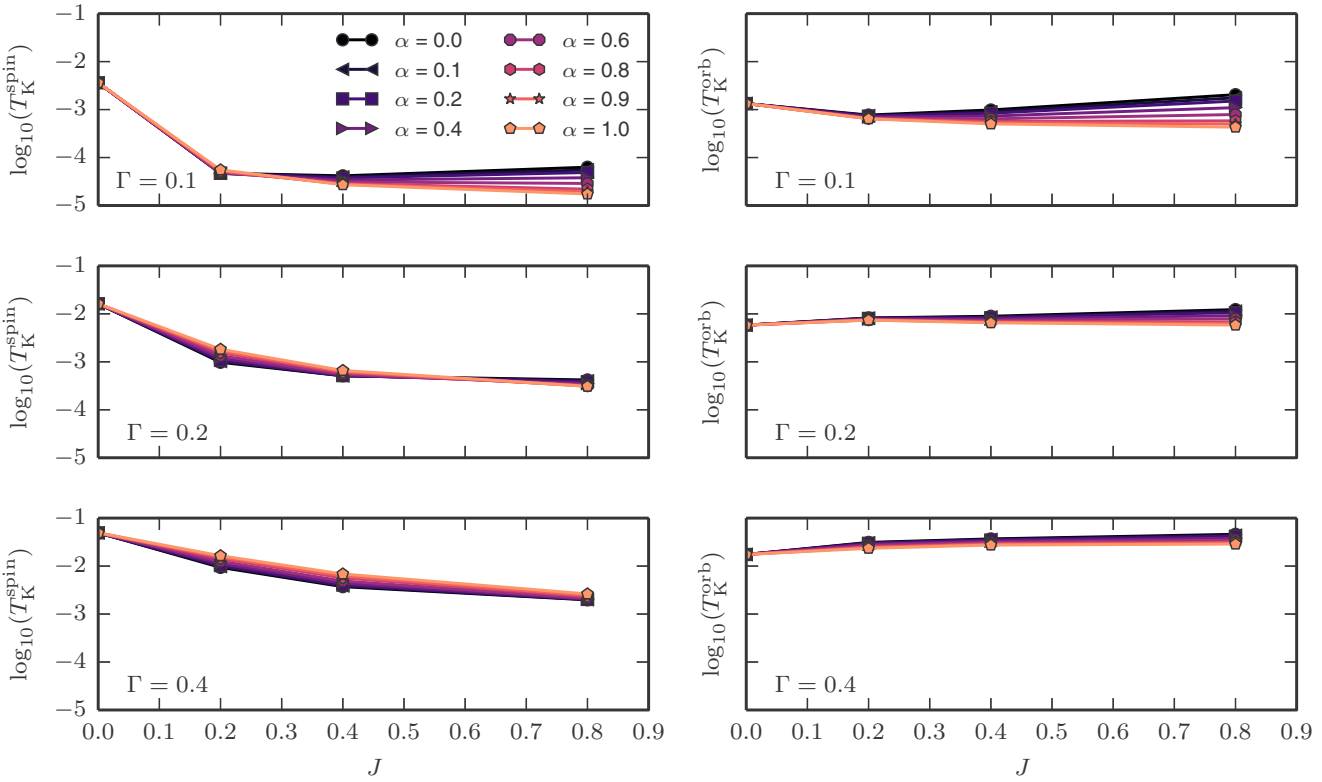

FIG. 7. Spin and orbital Kondo temperatures as a function of Hund's coupling J for different values of parameter α ($\alpha = 0$ DN interaction, $\alpha = 1$ Kanamori interaction). Model parameters are $U_{\text{eff}} = 2, N_d = 2$.

This result has the same form as the initial exchange interaction with an additional potential scattering term. A contribution from the scattering to the lower band edge is obtained in a similar fashion; the exchange term is the same, while the potential scattering term has an opposite sign and therefore cancels out that in Eq. (B9) since we have assumed a particle-hole symmetric conduction band. We recover the standard β function of the $S = 1/2$ Kondo model.

A similar approach can be used to tackle the multiorbital problem. We reproduce the scaling equations of Ref. [17] by applying the completeness relations for the fundamental representation of the spin and orbital moment operators (additionally one has to rescale the J_{ls} by a factor of 2). In the presence of the Hund's coupling and two electrons occupying the impurity, we have to take the $S = 1, L = 1$ representationw for the impurity spin and orbital moment operators. To calculate the scaling function an additional relation,

$$S_i S_j = \frac{2}{3}\delta_{ij} + \frac{i}{2}\epsilon_{ijk} S_k + Q^s_{ij}, \tag{B11}$$

has to be applied. ϵ_{ijk} tensor is determined by the commutator properties of the spin-1 operators $[S_i, S_j] = i\epsilon_{ijk} S_k$ and Q^s_{ij} are spin-quadrupole operators, which are absent from the original Kondo Hamiltonian. Spin-quadrupole operators are orthogonal to the spin operators hence they do not affect the spin scaling equations.

The scaling functions for a flat band, a general number of orbitals M occupied by two electrons, and $N = 2$ read

$$\beta_s = \frac{M({J_{ls}}^2 - M({J_{ls}}^2 + 2{J_s}^2)) - {J_{qs}}^2(M^2 + M - 2)}{2M^2}, \tag{B12}$$

$$\beta_l = \frac{1}{16}\big(-4{J_l}^2(M-2) - 3{J_{ls}}^2(M-2) - (M+2) \times\big(4{J_q}^2 + 8{J_{qs}}^2\big)\big), \tag{B13}$$

$$\beta_q = -\frac{1}{8}M(4J_l J_q + 8J_{ls}J_{qs}), \tag{B14}$$

$$\beta_{ls} = -\frac{J_{ls}(M(J_l(M-2) + 4J_s) + J_{qs}(M^2-4)) + J_q J_{qs} M(M+2)}{2M}, \tag{B15}$$

$$\beta_{qs} = -\frac{2J_{qs}M(J_l M + 4J_s) + J_{ls}M(J_{ls}(M-2) + 2J_q M) + {J_{qs}}^2(M^2 + 2M - 8)}{4M}. \tag{B16}$$

When $\alpha = 0, J_q = J_l, J_{qs} = J_{ls}$ and results are the same as obtained in Ref. [25] for the model with two electrons occupying the impurity and with a SU(M) orbital symmetry.

APPENDIX C: COMPARISON BETWEEN KANAMORI AND DWORIN-NARATH MODELS

Using parameter α [Eq. (5) in the main text] the impurity interaction can be continuously tuned between the Dworin-Narath ($\alpha = 0$) and the Kanamori ($\alpha = 1$) form. Even though the SO(3) orbital symmetry is dynamically restored to SU(3) at low energies and hence the behavior of the two models is similar there are quantitative differences that we illustrate here.

In Fig. 7 we present the spin and the orbit Kondo temperatures as a function of Hund's coupling for different values of α. Overall a qualitatively similar behavior is found. At small hybridizations up to an order of magnitude difference is found for large J. For small hybridization the spin Kondo temperature for Dworin-Narath is nonmonotonic at large J which is not the case for the Kanamori model. The calculated Kondo temperatures there differ by an order of magnitude between the two models which can be important for realistic DMFT calculations where the quantitative agreement with experiments is desired. Despite the overall similarity of the Dworin-Narath and Kanamori results, the more realistic Kanamori interaction needs to be used there.

[1] A. Georges, G. Kotliar, W. Krauth, and M. J. Rozenberg, Rev. Mod. Phys. **68**, 13 (1996).
[2] K. Haule and G. Kotliar, New J. Phys. **11**, 025021 (2009).
[3] P. Werner, E. Gull, M. Troyer, and A. J. Millis, Phys. Rev. Lett. **101**, 166405 (2008).
[4] J. Mravlje, M. Aichhorn, T. Miyake, K. Haule, G. Kotliar, and A. Georges, Phys. Rev. Lett. **106**, 096401 (2011).
[5] P. Hansmann, R. Arita, A. Toschi, S. Sakai, G. Sangiovanni, and K. Held, Phys. Rev. Lett. **104**, 197002 (2010).
[6] A. Georges, L. d. Medici, and J. Mravlje, Annu. Rev. Condens. Matter Phys. **4**, 137 (2013).
[7] Z. P. Yin, K. Haule, and G. Kotliar, Nat. Mater. **10**, 932 (2011).
[8] L. deMedici, in *Iron-Based Superconductivity*, Springer Series in Materials Science, Vol. 211, edited by P. D. Johnson, G. Xu, and W.-G. Yin (Springer International Publishing, Berlin, 2015), pp. 409–441.
[9] L. Fanfarillo and E. Bascones, Phys. Rev. B **92**, 075136 (2015).
[10] A. Hewson, *The Kondo Problem to Heavy Fermions* (Cambridge University Press, Cambridge, 1993).
[11] A. A. Khajetoorians, M. Valentyuk, M. Steinbrecher, T. Schlenk, A. Shick, J. Kolorenc, A. I. Lichtenstein, T. O. Wehling, R. Wiesendanger, and J. Wiebe, Nat. Nanotechnol. **10**, 958 (2015).
[12] H. T. Dang, M. dos Santos Dias, A. Liebsch, and S. Lounis, Phys. Rev. B **93**, 115123 (2016).
[13] L. de'Medici, J. Mravlje, and A. Georges, Phys. Rev. Lett. **107**, 256401 (2011).
[14] J. R. Schrieffer, J. Appl. Phys. **38**, 1143 (1967).
[15] C. Jayaprakash, H. R. Krishna-murthy, and J. W. Wilkins, Phys. Rev. Lett. **47**, 737 (1981).
[16] B. A. Jones and C. M. Varma, Phys. Rev. Lett. **58**, 843 (1987).
[17] Y. Kuramoto, Eur. Phys. J. B **5**, 457 (1998).
[18] H. Kusunose and K. Miyake, J. Phys. Soc. Jpn. **66**, 1180 (1997).
[19] S. Yotsuhashi, H. Kusunose, and K. Miyake, J. Phys. Soc. Jpn. **70**, 186 (2001).
[20] T. Pruschke and R. Bulla, Eur. Phys. J. B **44**, 217 (2005).
[21] A. H. Nevidomskyy and P. Coleman, Phys. Rev. Lett. **103**, 147205 (2009).
[22] Y. Nishikawa and A. C. Hewson, Phys. Rev. B **86**, 245131 (2012).
[23] L. Dworin and A. Narath, Phys. Rev. Lett. **25**, 1287 (1970).
[24] Z. P. Yin, K. Haule, and G. Kotliar, Phys. Rev. B **86**, 195141 (2012).
[25] C. Aron and G. Kotliar, Phys. Rev. B **91**, 041110 (2015).
[26] K. M. Stadler, Z. P. Yin, J. von Delft, G. Kotliar, and A. Weichselbaum, Phys. Rev. Lett. **115**, 136401 (2015).
[27] I. Okada and K. Yosida, Prog. Theor. Phys. **49**, 1483 (1973).
[28] J. Schrieffer and P. Wolff, Phys. Rev. **149**, 491 (1966).
[29] A. L. Fetter and J. D. Walecka, *Quantum Theory of Many-particle Systems* (Courier Corporation, North Chelmsford, 2003).
[30] L. de Leo, Ph.D thesis, SISSA, 2004.
[31] P. W. Anderson, J. Phys. C: Solid State Phys. **3**, 2436 (1970).
[32] T. Kuzmenko, K. Kikoin, and Y. Avishai, Phys. Rev. Lett. **89**, 156602 (2002).
[33] K. Kikoin and Y. Avishai, Phys. Rev. B **65**, 115329 (2002).
[34] L. Borda, G. Zaránd, W. Hofstetter, B. I. Halperin, and J. von Delft, Phys. Rev. Lett. **90**, 026602 (2003).
[35] K. Kikoin, M. N. Kiselev, and M. R. Wegewijs, Phys. Rev. Lett. **96**, 176801 (2006).
[36] A. J. Keller, S. Amasha, I. Weymann, C. P. Moca, I. G. Rau, J. A. Katine, H. Shtrikman, G. Zaránd, and D. Goldhaber-Gordon, Nat. Phys. **10**, 145 (2014).
[37] R. Žitko, Computer code NRG LJUBLJANA, nrgljubljana.ijs.si/.
[38] The precise value depends on the parameters. The dominant exponential dependence on the Coulomb interaction parameters is, however, the same for the spin and orbital Kondo temperature.
[39] L. Hirst, Adv. Phys. **27**, 231 (1978).
[40] P. Cvitanovic, Phys. Rev. D **14**, 1536 (1976).
[41] D. A. Varshalovich, *Quantum Theory of Angular Momentum: Irreducible Tensors, Spherical Harmonics, Vector Coupling Coefficients, 3 nj Symbols* (World Scientific, Singapore/Philadelphia, 1989).
[42] L. C. Biedenharn and J. D. Louck, *Angular Momentum in Quantum Physics* (Cambridge University Press, Cambridge, 1984).